
Quantifying Emergence in Large Language Models

Hang Chen

School of Computer Science and Technology
Xi'an Jiaotong University
albert2123@stu.xjtu.edu.cn

Xinyu Yang

School of Computer Science and Technology
Xi'an Jiaotong University
yxyphd@mail.xjtu.edu.cn

Jiaying Zhu

School of Computer Science and Engineering
The Chinese University of Hong Kong
zhujiy0725@cse.cuhk.edu.hk

Wenya Wang*

School of Computer Science and Engineering
Nanyang Technological University
wangwy@ntu.edu.sg

Abstract

Emergence, broadly conceptualized as the “intelligent” behaviors of LLMs, has recently been studied and proved challenging to quantify due to the lack of a measurable definition. Most commonly, it has been estimated statistically through model performances across extensive datasets and tasks, which consumes significant resources. In addition, such estimation is difficult to interpret and may not accurately reflect the models’ intrinsic emergence. In this work, we propose a quantifiable solution for estimating emergence. Inspired by emergentism in dynamics, we quantify the strength of emergence by comparing the entropy reduction of the macroscopic (semantic) level with that of the microscopic (token) level, both of which are derived from the representations within the transformer block. Using a low-cost estimator, our quantification method demonstrates consistent behaviors across a suite of LMs (GPT-2, GEMMA, etc.) under both in-context learning (ICL) and natural sentences. Empirical results show that (1) our method gives consistent measurements which align with existing observations based on performance metrics, validating the effectiveness of our emergence quantification; (2) our proposed metric uncovers novel emergence patterns such as the correlations between the variance of our metric and the number of “shots” in ICL, which further suggests a new way of interpreting hallucinations in LLMs; (3) we offer a potential solution towards estimating the emergence of larger and closed-resource LMs via smaller LMs like GPT-2. Our codes are available at: <https://github.com/Zodiark-ch/Emergence-of-LLMs/>.

1 Introduction

Emergence, one of the most enigmatic and elusive attributes of LLMs [31, 24, 26], is broadly conceptualized as a phenomenon of “high-level intelligence” that becomes observable only when the model reaches a sufficiently large size. It encompasses the comprehension of abstract concepts [33], complex language skills [2], natural human interactions [18], instructions following [36], generalization out of domains [12], and even unanticipated patterns like hallucinations [22].

To measure emergence, existing research adopts a compromised approximation: evaluating the performance of a model across extensive datasets and tasks under a pre-defined performance metric such as accuracy, F1-score, etc. For example, recent work [24], under the linear and continuous metrics, has demonstrated that emergence is not “unreasonable like magic” but rather can be extrapolated

*Corresponding author

from smaller models. However, these evaluations pose three main limitations. Firstly, evaluating emergence through performance metrics across numerous tasks and datasets is time-consuming and resource-intensive. Secondly, it does not provide an internal explanation at a finer-grained level such as specific tokens or model components to better understand the mechanism. Thirdly, pre-defined performance metrics may not correlate precisely with the strength of emergence, especially when the metric fails to capture the creativity or flexibility of LM-generated answers.

Despite these limitations, research into the intrinsic nature of emergence still remains a highly under-explored area. Therefore, our work is dedicated to proposing a quantifiable definition of emergence in LLMs and a low-cost implementation. Specifically, motivated by theories in emergentism [23, 13, 14], we model LLMs as a Markov process and define the emergence strength between internal transformer layers from the perspective of information theory. Concisely, emergence can be described as a process where **the entropy reduction of the entire sequence exceeds the entropy reduction of individual tokens**. To compute entropy reduction, we resort to mutual information between successive transformer layers and adopt a practically effective estimation algorithm proposed in [6] which is suitable for high-dimensional continuous representations.

To demonstrate the effectiveness and validity of our proposed emergence metric, we devise a suite of comprehensive experiments encompassing two different scenarios. In the first scenario, we target on *emergence in “shots”* and curate a group of synthetic datasets under the in-context learning (ICL) setting to account for different numbers of demonstrations (“shots”) in ICL as well as different context domains. In the second scenario, we focus on *emergence in sentences* and collect two benchmark datasets consisting of real-world natural language questions/answers. Under both scenarios, we experiment with different LMs including GPT-2 [21], GEMMA [28], and OpenLlama [10] to study the emergence patterns. Interestingly, we observe robust phenomenon across these LMs when quantifying their emergence, which align with existing findings based on commonly used performance metrics. For instance, an increase in model size and context length correlates with higher emergence. Additionally, novel patterns are detected, e.g., sequences with ICL-style “shots” display distinct emergence patterns compared to natural sequences.

On top of that, our methodology offers underlying insights applicable to several research areas within LLMs: **1)** By estimating the emergence strength across numerous LLMs, empirical formulas about emergence akin to Scaling Laws [3] can be developed. **2)** Our research indicates a potential connection between the high variations of emergence strength and occurrence of hallucinations in LLMs, paving a future direction towards hallucination detection via models’ internal mechanisms. **3)** Our method demonstrates the feasibility of using smaller LMs like GPT-2 to estimate the emergence capabilities of extremely large and close-resource LMs like GPT-4 [1] with low computational cost. Overall, our contributions could be summarized below:

- To our best knowledge, this is the first work to theoretically quantify the emergence strength in LLMs and provide a rather low-cost solution to estimate the emergence strength.
- Extensive experiments under the settings of ICL and natural sentences have uncovered numerous inspiring emergence patterns, aligning with and beyond existing findings.
- Our experimental findings further potentially support the feasibility and encourage the exploration of a wide range of applications of greater value within the scope of LLMs.

2 Related Work

Initially, the emergence capabilities of LLMs were described as “*Emergence is when quantitative changes in a system result in qualitative changes in behavior*” [31]. This description indicates that such capabilities are abrupt and unpredictable — eluding extrapolation from smaller-scale models. Therefore, a prevalent approach involves adopting extensive datasets and tasks, then evaluating the models’ performance via metrics—such as accuracy, F1 score, and Exact Match (EM)—which depend on the specific datasets and tasks, and using these metrics to statistically elucidate the emergence capabilities. To date, numerous studies [26, 18, 35, 17, 7, 9] have continued this approach and have observed such an abrupt phenomenon.

More recently, several studies have demonstrated both theoretically and experimentally that emergence capabilities can be observed as smooth and continuous phenomenon. [2] integrated text pieces with language skills into a bipartite random graph thus employing Scaling Laws to model emergence

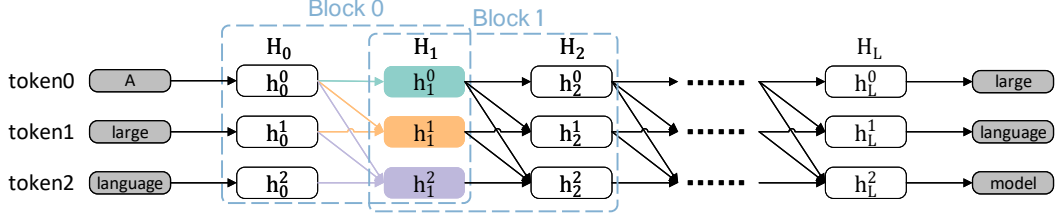


Figure 1: The analogy of NTP to Markov process. Taking the output representation of token2 in Block 0 (h_0^2) as an example, which receives information from input representations of h_0^0 , h_0^1 , and h_0^2 , satisfying $p_{h_{i+1}^2|H_i^{\leq t}} = p_{h_{i+1}^2|h_i^0, h_i^1, h_i^2}$.

properties ranging from smaller to larger models. [24] proposed that the abrupt nature of emergence derives from nonlinear or discrete metrics, and experimentally confirmed that when metrics are linear and continuous, the emergence capabilities appear smooth and predictable.

Despite a novel pathway for defining and quantifying the emergence in LLMs pioneered by us, our empirical investigations substantiate these previous viewpoints: strength of emergence does scale continuously with model size, datasets, prompt form, and context.

3 Method

3.1 How to Model Emergence in LLMs

In this paper², we identify the transformer block as the fundamental unit for observations of robust emergence phenomenon. Specifically, we employ $l = 0, 1, \dots, L - 1$ to index transformer blocks within a language model, where L represents the total number of blocks. For instance, GPT-2 XL (1.6B parameters)³ comprises 12 blocks ($L = 12$), and Gemma-2B⁴ totals 18 blocks ($L = 18$). Without loss of generality, we hypothesize that the process of token representations passing through transformer blocks constitutes a Markov process. Specifically, For any transformer block l , given an input sequence of token length T and hidden state dimension D , the input representation is given by $H_l = \{h_l^0, h_l^1, h_l^2, \dots, h_l^{T-1}\}$ and the output representation is $H_{l+1} = \{h_{l+1}^0, h_{l+1}^1, h_{l+1}^2, \dots, h_{l+1}^{T-1}\}$, where $H \in \mathbb{R}^{T \times D}$ and $h^t \in \mathbb{R}^{1 \times D}$.

Hypothesis 1 (Markov Process Analogy). *The Next Token Prediction (NTP) mechanism undergoes a Markovian stochastic process following a transition probability of any h_{i+1}^t with $p_{h_{i+1}^t|h_i^0, h_i^1, h_i^2, \dots, h_i^t}$, simply denoted by $p_{h_{i+1}^t|H_i^{\leq t}}$.*

Hypothesis 1 omits normalization layers, MLP layers, and residual structures between transformer blocks, and thus the output of l -th block is directly considered as the input to $l + 1$ -th block (H_{l+1}), as shown in Figure 1. This omission is supported by previous research [30] which shows that the flow of information in LLMs is largely concentrated within the attention layers of transformer architecture.

Accordingly, we could categorize token variables within each sequence into two distinct categories: **microscopic (micro) variables** and **macroscopic (macro) variables**. A micro variable refers to a token which is solely influenced by a single token as the input. For instance, h^0 satisfies $p_{h_{l+1}^0|h_l^0}$. Whereas macro variables aggregate information from all micro variables and thus encompass tokens which are influenced by all the tokens within the sequence as the input. An example could be h_{l+1}^{T-1} which satisfies $p_{h_{l+1}^{T-1}|h_l^0, h_l^1, \dots, h_l^{T-1}}$. In summary, the NTP mechanism can be viewed as a behavior that increasingly coarsens from the most micro to the most macro scale.

With emergence described as “when quantitative changes in a system result in qualitative changes in behavior” [31], and the introduction of micro/macro variables, the definition within emergentism can

²Please note that this paper addresses decoder-only autoregressive language models, while other language models that do not meet the requirements, such as BERT [11] family, are not considered within the scope.

³<https://huggingface.co/openai-community/gpt2-xl>

⁴<https://huggingface.co/google/gemma-2b>

be articulated as “Emergence is when micro changes in a fine-grained system result in macro changes in the collective perspective.” Succinctly, phenomenon observable at a macro level, yet unobservable at a micro level during a dynamic process, are abstracted as emergence.

Example 1. Given T binary tokens $H_l = \{h_l^0, h_l^1, \dots, h_l^{T-1}\} \in \{0, 1\}^T$ as inputs, for simplicity, we assume all variables are micro variables: $\forall h_{l+1}^t \in H_{l+1}$ satisfies $p_{h_{l+1}^t|h_l^t}$ (the simplest Markov process, and in the subsequent of this Example, we use p to simply denote this transition probability). The output representations are also binary, i.e., $H_{l+1} \in \{0, 1\}^T$. We assume an evolution rule which enables the parity of the sum of all output variables equal to the sum of all inputs with probability γ . If H_l satisfies the uniform distribution, the evolution rule entails the probability of the output H_{l+1} :

$$p(H_{l+1}|H_l) = \begin{cases} \frac{\gamma}{2^{T-1}}, & \text{if } \bigoplus_{t=0}^{T-1} h_{l+1}^t = \bigoplus_{t=0}^{T-1} h_l^t \\ \frac{1-\gamma}{2^{T-1}}, & \text{otherwise} \end{cases} \quad (1)$$

where $\bigoplus_{t=0}^{T-1} h_l^t := 1$ if $\sum_{t=0}^{T-1} h_l^t$ is even and $\bigoplus_{t=0}^{T-1} h_l^t := 0$ if odd. For example, if $H_l = \{0, 0, 0\}$, H_{l+1} can be one of $\{0, 0, 0\}, \{0, 1, 1\}, \{1, 0, 1\}, \{1, 1, 0\}$ with probability γ , leading to $\frac{\gamma}{2^{3-1}}$ chance for each candidate above. Each of the remaining value for H_{l+1} has probability $\frac{1-\gamma}{2^{3-1}}$.

With the assumption of micro dependency $p_{h_{l+1}^t|h_l^t}$, we can derive the distribution of a **micro variable** as $p(h_{l+1}^t=0|h_l^t) = p(h_{l+1}^t=1|h_l^t) = 0.5$. Finally, let h^{ma} be the macro variable with $h^{ma} = \bigoplus_{t=0}^{T-1} h_l^t$. Then the distribution of the **macro variable** becomes:

$$p(h_{l+1}^{ma}|h_l^{ma}) = \begin{cases} \gamma, & \text{when } h_{l+1}^{ma} = h_l^{ma} \\ 1 - \gamma, & \text{when } h_{l+1}^{ma} \neq h_l^{ma} \end{cases} \quad (2)$$

Example 1 elucidates an interesting phenomenon known as emergence: The macro variable h^{ma} is not induced by any individual micro variable but a collective of them. As a result, it shows different phenomenon from any micro variable. Moreover, we note that the same evolution rule applies to both micro and macro variables. This is known as **Supervenience Hypothesis** [4, 5] in emergentism:

Hypothesis 2 (Supervenience). *When the properties of the micro-level mechanisms of a system are fixed, so are the properties of all its macro levels.*

Hypothesis 2 explicates that the “new phenomenon” in macro systems does not materialize *ex nihilo*. The micro level is causally and mechanically complete, and there is no room left for any causal and mechanical contribution at the macro level. In other words, the phenomenon that emerged in macro has irreducible causal and mechanical power in practice but not in principle, all because the micro level is too fine-grained to observe such a phenomenon.

Given the Supervenience hypothesis and motivated by more endeavors about emergentism [23, 13, 14], we can define emergence in LLMs as:

Definition 1 (Emergence in LLMs). *For any transformer block l in a LLM, let h_l^{ma} be the **macro variable** (h_l^{ma} satisfies $p_{h_{l+1}^{ma}|H \leq T}$) and let h_l^{mi} be the **micro variable** (h_l^{mi} satisfies $p_{h_{l+1}^{mi}|h_l^{mi}}$), the strength of emergence in block l can be described as:*

$$E(l) = MI(h_{l+1}^{ma}, h_l^{ma}) - \frac{1}{T} \sum_{t=0}^{T-1} MI(h_{l+1}^{mi,t}, h_l^{mi,t}) \quad (3)$$

where $MI(\cdot, \cdot)$ represents the mutual information.

Definition 1 describes how to estimate the strength of emergence. To illustrate, suppose an input sequence contains three tokens ‘large language model’, with their representations at the l th block denoted as $H_l = \{h_l^0, h_l^1, h_l^2\}$. To compute the mutual information at the micro level, we need to make sure each micro token is positioned at the beginning of the sequence to avoid the influence from other tokens due to the Markov process in Hypothesis 1. Specifically, we obtain the first micro variable $\{h_l^{mi,0}\}_{l=0}^{L-1}$ where $h_l^{mi,0} = h_l^0$ corresponds to ‘large’ derived by going through the transformer model for the input ‘large language model’. The second micro variable $\{h_l^{mi,1}\}_{l=0}^{L-1}$ corresponds to ‘language’ given by going through the transformer model one more time for the modified input ‘language model’. The third micro variable proceeds in a similar manner by removing

the first two tokens in the original input. These modified inputs ensure that each micro variable only depends on itself in the previous block. Meanwhile, the macro variable $\{h_l^{ma}\}_{l=0}^{L-1}$ is given by $h_l^{ma} = h_l^2$ for the original input sequence ‘large language model’. Finally, we have $E(l) = MI(h_{l+1}^{ma}, h_l^{ma}) - \frac{1}{3}(MI(h_{l+1}^{mi,0}, h_l^{mi,0}) + MI(h_{l+1}^{mi,1}, h_l^{mi,1}) + MI(h_{l+1}^{mi,2}, h_l^{mi,2}))$.

Notably, We measure the emergence by comparing the macro changes with the micro changes across blocks, instead of directly computing $MI(h_l^{ma}, h_l^{mi})$ at the same block, justified by the Supervenience hypothesis which posits that under the same state, micro and macro variables do not exhibit emergent properties. We use Example 2 to explain why the mutual information between macro variables and micro variables is different:

Example 2. Continuing from Example 1, for simplicity, we assume $\gamma=1$, $T=3$. Assuming block l undergoes a uniform distribution, we have $p(h_l^{ma}=0) = p(h_l^{ma}=1) = 0.5$ and $p(h_l^{mi,t}=0) = p(h_l^{mi,t}=1) = 0.5$. Without loss of generality, let’s assume $h_l^{ma} = 0$ and $h_l^{mi,t} = 0$. According to Example 1, we have $p(h_{l+1}^{mi,t}=0|h_l^{mi,t}) = p(h_{l+1}^{mi,t}=1|h_l^{mi,t}) = 0.5$. On the contrary, $p(h_{l+1}^{ma} = 0|h_l^{ma}) = \gamma = 1$. Hence, the emergence value becomes $E(l) = 1 - \frac{1}{3}(0 + 0 + 0) = 1$.

Example 2 elucidates that the difference in mutual information stems from a coarse-graining that transitions from individual elements (micro) to an aggregate whole (macro). From an information theory perspective, $E(l) > 0$ indicates that when the function of transformer block l results in a higher reduction of uncertainty (entropy) on the whole sequence (macro variable) compared to the individual tokens (micro variables), there is a higher chance of observing an emergence phenomenon.

Consequently, the strength of emergence can be briefly understood as **“how confidence with which a language model, based on previous tokens, definitely predicts the next token with a lower entropy in semantics”**.

3.2 How to Estimate Emergence in LLMs?

It is not feasible to directly compute the mutual information in Eq. 3 using Kullback-Leibler (KL) divergence, as the input lies in a high-dimensional continuous space. To address that, we resort to an approximation method using mean values proposed in [6]:

$$D_{KL}(\mathbb{P}||\mathbb{Q}) = \limsup_{f:\Omega \rightarrow \mathbb{R}} E_{\mathbb{P}}[f] - \log(E_{\mathbb{Q}}[e^f]) \quad (4)$$

where f represents a function that maps \mathbb{Q} to Gibbs distribution by $dG = \frac{1}{Z} e^f d\mathbb{Q}$, where $Z = E_{\mathbb{Q}}[e^f]$. Naturally, f can be a neural model. Thereby, Equation 4 can be equivalently represented as optimizing the error function \mathcal{L} :

$$\mathcal{L} = \frac{1}{B} \sum_{b=1}^B (f_{\theta}(x^b||y^b)) - \log\left(\frac{1}{B} \sum_{b=1}^B e^{f_{\theta}(x^b||y^{i \neq b})}\right) \quad (5)$$

where θ denotes the parameters for f , $||$ denotes the concatenation operation and B is the batch size. $x, y \in \mathbb{R}^D$ are two inputs for computing the mutual information $MI(x, y)$. $x^b||y^b$ corresponds to sampling from the joint distribution P_{XY} , while $x^b||y^{i \neq b}$ corresponds to sampling from the marginal distribution P_X and P_Y ⁵. When \mathcal{L} converges to the minimum $\hat{\mathcal{L}}$, we can obtain the final estimated mutual information as $MI(x, y) = -\log_2^e * \hat{\mathcal{L}}$. (More details and proofs are shown in [6].)

To get the emergence value $E(l)$ in Eq. 3, we compute $MI(h_{l+1}^{ma}, h_l^{ma})$ by replacing x^b and y^b in Eq. 5 with $h_{l+1,s}^{ma}$ and $h_{l,s}^{ma}$ obtained by applying the LM to the same input sequence s , whereas replacing $y^{i \neq b}$ with $h_{l,s'}^{ma}$ using a different sequence $s' \neq s$. Similar operations apply when computing $MI(h_{l+1}^{mi,t}, h_l^{mi,t})$. (Refer to Appendix A for a complete algorithm for estimating the emergence.)

3.3 Implementation

We examine the emergence strength of LLMs under two distinct settings: **ICL** with few-shot examples and **natural sentences** without demonstrations. For both settings, our algorithm requires

⁵In our implementation, the batch size was increased to encompass the entirety of the sample set to ensure the rationality of P_{XY} , P_X and P_Y .

that the number of samples is sufficiently large (over 300k) to provide a good estimate of the mutual information. Meanwhile, the length of each sequence within a dataset should be kept the same to facilitate position-wise observation and meaningful computation.

Due to resource constraints, our comparative analysis is limited to GPT2-large (812M)⁶, GPT2-XL (1.61B), GEMMA (2.51B), and OpenLlama (3B)⁷ models. Fortunately, this parameter range is sufficient to observe variations and regularities of the emergence phenomenon. For those LLMs with extremely large size or closed resource (e.g., GPT-4, Claude3, etc.), we design another strategy that enables their emergence evaluations as shown in Section 5.2. All computational experiments can be conducted on **one** NVIDIA GeForce RTX 3090 GPU⁸. The estimator f in Eq. 3 is a model of a 10-layer neural network comprising linear layers and leaky ReLU activation functions, where each linear layer’s output dimension was half of its input dimension. We set the batch size to 300,000 to ensure the stability of the sampling distribution, thereby guaranteeing robust results. Additionally, the learning rate was initially set at 1e-4 and was polynomially decayed to 1e-8 within 10k epochs.

4 Emergence in ICL

In this section, we focus on the performance of LLMs’ emergence in ICL, specifically examining the strength of emergence in the span of shots. Since existing datasets (e.g., SST-2 [25], AGNews [38], and EmoC [8]) do not meet the requirement of the same sequence length, we synthesized a set of simple few-shot samples having token length and positions aligned across different sequences. We curate three different datasets encompassing three different domains, each containing sequences of few-shot single-token entities with commas:

- **Country:** We select 25 countries from the Vocabulary as *entities*, each represented by 1 token (e.g., ‘Canada’, ‘Russia’). Each shot consists of one *entity* followed by a *comma*, totaling 2 tokens. We constructed $25 * 24 * 23 * 22 = 303,600^9$ input sequences, each comprising 8 tokens (4 different shots), such as “France, Mexico, Egypt, Russia.”
- **Animal:** Similarly, we select 16 animals as *entities*, and construct $16 * 15 * 14 * 13 * 12 = 524160$ input sequences comprising 10 tokens (5 different shots), such as “Fox, Pig, Penguin, Rabbit, Cock.”
- **Color:** We select 15 colors as *entities*, and construct 360360 samples comprising 10 tokens (5 different shots), such as “red, orange, yellow, green, blue.”

In the experiment, we observe that each *entity*, treated as a micro variable (i.e., the first token), produces similar mutual information across different positions. Consequently, in this section, we only use the *entity* in the first position to compute the mutual information to approximate the mean of all micro variables. Moreover, $E(l)$ also acts analogously in each block, so we utilize the mean of $\{E(l)\}_{l=0}^{L-1}$ to show the emergence strength. By varying the position t of the macro variable (last token in a sequence), we use the following equation to compute the emergence strength at length t :

$$\hat{E}(t) = \frac{1}{L} \sum_{l=0}^{L-1} E(l)_{ma=t-1} = \frac{1}{L} \sum_{l=0}^{L-1} (MI(h_{l+1}^{t-1}, h_l^{t-1}) - MI(h_{l+1}^0, h_l^0)) \quad (6)$$

4.1 Finding 1: Emergence Increases by Shots but Stabilizes within a Shot.

Figure 2 indicates the emergence strength across the first 4 shots¹⁰, based on which 3 observations can be derived:

- The emergence escalates with an increasing number of shots within a certain range. **(O1)**

⁶<https://huggingface.co/openai-community/gpt2-large>

⁷https://huggingface.co/openlm-research/open_llama_3b

⁸For easy deployment, we split the representations of LLMs into several 768-dimension segments and the final representation is the mean of these segments.

⁹The number of shots is decided to ensure the number of combinations in each category is over 300000.

¹⁰The whole record of every token’s mutual information is detailed in Table 5, showing the example of GPT2-XL on the Animal category.

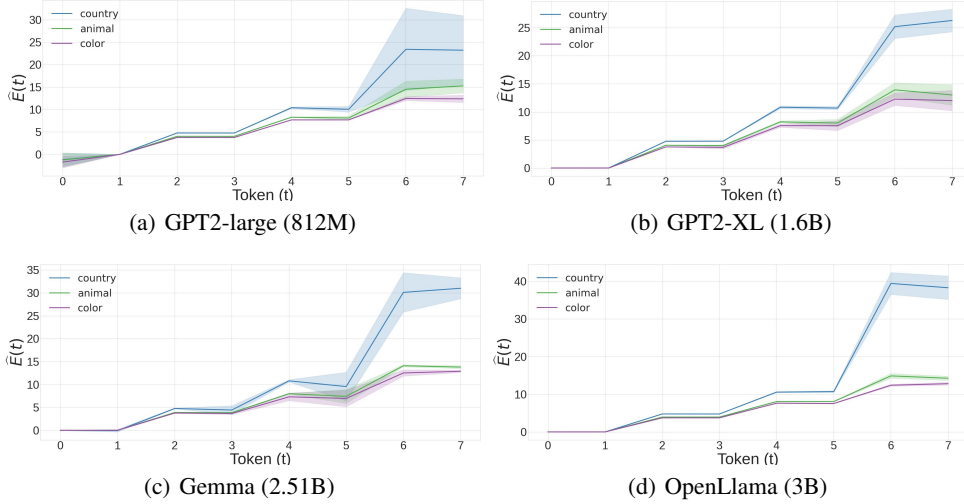


Figure 2: $\hat{E}(t)$ on 3 datasets with mean and variance.

- The standard deviation of emergence increases when the number of shots increases. **(O2)**
- Tokens within the same shot exhibit approximately equivalent strength of emergence. **(O3)**

O1 highlights the role of “shot” in ICL: an increased number of shots enhances the confidence in predicting the next token. This observation corroborates substantial research that intuitively and experimentally explores ICL [19, 20, 32, 34, 15, 27]. Yet, the contribution of shots is not infinitely amplified. Table 3 indicates that the emergence tends to saturate beyond the 7-th shot.

O2 indicates that emergence becomes unstable as the number of shots increases. To further study this observation, we explicitly report the emergence strength and standard deviation in Table 1 and compute the accuracy of the generations¹¹ spanning over different number of shots. As can be seen from rows 1-9 of Table 1, as emergence strength ceases to grow and the variance reaches to the peak, the LM displays a higher probability of generating inaccurate responses. From a closer look, we discover that oftentimes, the LM fails to generate new entities due to “error repetition” (explanations and some examples can be found in Appendix B.3). This is aligned with existing study [37] related to hallucination. Specifically, LLMs struggle to correct itself subsequently after generating an erroneous output, consequently obstructing the emergence of correct new information, resulting in stagnation and fluctuation in emergence evaluation.

However, this should not be confused with the power of ICL in exploiting more complex patterns effectively with more “shots” as the input. Different from the above observation, an increasing number of shots tends to bring higher accuracies under more complex scenarios. As shown in rows 10-15 of Table 1, we design four challenging tasks: ‘Asia’ and ‘Europe’ only provide countries in Asia and Europe, respectively, as input demonstrations; ‘Size’ contains animals arranged by size from smaller to larger; ‘Alphabet’ sorts the entities alphabetically based on the first letter. The accuracy results indicate that LLMs

Emergence Statistics by each shot							
Statistics	shot1	shot2	shot3	shot4	shot5	shot6	shot7
strength	4.013	8.34	12.95	26.81	61.59	82.49	71.52
SD	<0.01	0.59	0.84	2.61	6.59	7.22	7.05
Accuracy of LLMs outputs given shots (%)							
dataset	shot1	shot2	shot3	shot4	shot5	shot6	shot7
country	0	54.15	74.29	88.47	46.21	21.59	22.68
animal	0	44.51	69.43	76.19	64.19	36.14	33.54
color	0	37.49	66.51	72.18	73.16	46.95	38.49
Accuracy in 4 complex pattern given shots (%)							
pattern	shot1	shot2	shot3	shot4	shot5	shot6	shot7
Asia	0.35	3.27	4.26	15.29	34.72	84.53	79.16
Europe	3.75	8.29	11.16	24.68	49.36	89.38	89.51
Size	4.59	2.94	6.43	7.29	7.16	26.46	34.19
Alphabet	0.11	1.26	1.47	39.16	69.17	54.91	18.67

Table 1: The relationship between the accuracy of GPT2-XL outputs and emergence statistics by each shot in 3 categories.

¹¹We randomly sample a total of $N = 1000$ samples and regard the generation to be correct if the generated entity belongs to the corresponding domain of the dataset (country, animal or color) and is not repetitive.

require more shots to capture complex patterns compared to simple patterns. Thus, it prompts us to conjecture if the stagnation and fluctuations in the emergence are associated with another hallucination: with excessive shots, LLMs may perceive more complex patterns beyond the surface (or even actual) appearance. In short, The correlation between emergence variance and hallucination would offer novel insights into the future development of hallucination detection and mitigation.

To validate **O3**, we compare the emergence strength ending with different positions (*entity* or *comma*) and vary the number of shots. Figure 4 demonstrates that the emergence strength remains consistent within each shot regardless of the position.

4.2 Finding 2: Emergence Is Associated with the Model, Dataset, Task, and Prompt.

To investigate the influence of different factors on emergence strength, we treat the performance of GPT2-XL on the “country” dataset as a baseline and implement a series of ablation studies. Appendix C details the variations when different factors change. It was observed that the emergence increases with the size of the model and the length of the token. This corroborates existing observational conclusions [31, 26] that emergence is more likely to occur in scenarios with a larger number of model parameters and richer contextual information. In addition, our study also identifies variations in emergence depend on the semantics, task, and prompt form, which also resonates with findings from prior research [18, 35, 17].

5 Emergence in Sentences and Datasets

The emergence of natural sentences is also a concern of our study. We randomly select 300,000 sequences, each consisting of 8 tokens, from OpenOrca [16] and OpenHermes [29], respectively. OpenOrca and OpenHermes are both large-scale, multi-domain QA datasets. These sequences were selected to ensure that the first token in each sequence is the actual beginning of a sentence.

In our experiments, we observe potential discrepancies in mutual information for individual tokens at different positions within a sentence (i.e., micro mechanisms in different positions are not consistent). These discrepancies are detailed in Appendix D). Consequently, for the mutual information of micro-level variables, we adhere to Equation 3 which averages the micro MI at each position:

$$\hat{E}(t) = \frac{1}{L} \sum_{l=0}^{L-1} E(l)_{ma=t-1} = \frac{1}{L} \sum_{l=0}^{L-1} (MI(h_{l+1}^{t-1}, h_l^{t-1}) - \frac{1}{t} \sum_{m=0}^{t-1} MI(h_{l+1}^m, h_l^m)) \quad (7)$$

5.1 Finding 3: Emergence Increases by Tokens in Natural Sentences

Figure 3 presents the performance of GPT2-large (0.8B), GPT2-XL (1B), GEMMA (2B), and OpenLlama (3B) on OpenOrca and OpenHermes datasets. We observe that emergence increases with the number of tokens, as natural sentences often possess sufficiently explicit semantics to provide confidence in predicting the next tokens. However, different datasets exhibit varying levels of emergence. Given the substantial size of our sample (300k), we attribute these variations primarily to differences in domain-specific characteristics. Moreover, we observed that the strength of emergence is averagely lower than that of ICL in Section 4.1. This highlights that ICL does enable LLMs to more effectively ascertain the next tokens compared to natural sentences. Concurrently, disparate performances observed across the two datasets and three model families suggest that the domain of the training data and preprocessing methodologies are likely critical factors, as further supported by the evaluations of individual tokens at different sentence positions elaborated in Appendix D. For instance, GPT2-large and GPT2-XL, which share the same dataset (40GB WebText), preprocessing methods, and model architecture, exhibit a common characteristic: the mutual information of the first token is consistently lower than the average mutual information of micro-level variables.

5.2 Finding 4: Texts Generated from LLMs and Humans Exhibit Different Emergence

Motivated by the robust emergence in natural sentences in Section 5.1, we seek to measure the differences in text generated by larger language models compared to human texts, as well as the variations among these LLMs themselves. Specifically, we use questions from OpenHermes as inputs

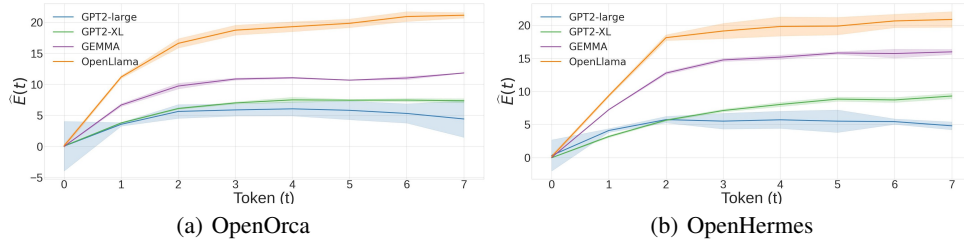


Figure 3: $\hat{E}(t)$ on 2 datasets.

Text+Estimator	token0	token1	token2	token3	token4	token5	token6	token7	token8
Human+GPT2-XL	10.9	16.9	18.6	19.5	19.5	19.7	19.6	19.5	19.4
Human+GEMMA	9.5	16.8	22.4	24.3	24.0	25.3	24.6	25.0	25.9
GPT4+GPT2-XL	11.3	18.8	23.5	27.2	34.5	37.2	39.2	39.5	39.2
GPT4+GEMMA	12.1	20.5	25.1	31.6	36.3	39.9	40.4	39.5	40.6
Claude3-opus+GPT2-XL	12.6	21.8	26.6	29.5	36.8	39.8	42.6	45.2	45.3
Claude3-sonnet+GPT2-XL	11.4	17.4	24.8	28.5	32.5	36.5	36.1	36.2	36.2
Llama3 (70B)+GPT2-XL	11.2	18.1	23.6	24.5	28.5	32.6	36.5	36.8	36.6

Table 2: Emergence in texts generated from human and popular LLMs. “text” refers to the party that generates the text. “Estimator” refers to the LM used to transform the text into representations and estimates the emergence strength using f described in Section 3.2.

and collect responses by invoking the APIs of GPT-4, Claude3-opus, Claude3-sonnet, and Llama3. These responses were subjected to the same data processing methods described in Section 5. To evaluate these extremely large and closed-source language models, we implement a 3-step strategy:

Step 1: Collect the answers from these LLMs (or humans) via the questions from the OpenHermes.

Step 2: Following the data processing in Section 5, we format these answers into input sequences of 8 tokens and obtained their representations using smaller LMs (e.g., GPT-2, GEMMA).

Step 3: These representations were then processed through an estimator to calculate the mutual information introduced in Section 3.2, thereby determining the emergence strengths of these answers via Equation 7.

Table 2 illustrates an interesting phenomenon: LLM-generated texts exhibited substantially greater emergence strength than human texts. This observation is intuitive—given that LLMs aim to generate tokens with the highest probability, naturally resulting in greater entropy reduction.

Another observation is that the text generated by different LLMs (GPT-4, Claude3, and Llama3) displays variations in emergence strengths. Significant differences are observed not only in the maximum strength of the emergence but also in the patterns of growth. Without actually computing the transformer representations of the target LLMs, these findings open a promising path towards estimating the emergence capability from extremely large and closed-source LMs without expensive computational costs.

6 Limitations

We observe that LLMs exhibit a trend where larger model sizes correlate with higher emergence. This naturally prompts us to explore the empirical law between model parameters, dataset size, and emergence strength as Scaling Laws [3]. However, due to limited computational resources, we provide a preliminary study on smaller LMs and introduce a novel way of estimating the emergence of large LMs. Therefore, we would like to reiterate our contribution: pioneering the path for quantifying emergence in LLMs. Nonetheless, there still remains room for exploration such as a robust and efficient way of computing mutual information with higher dimensions and varied token lengths.

7 Conclusion

In this paper, we propose a quantification method to approximate the essential nature of the emergence of LLMs. Firstly, we provide a quantifiable definition of emergence and a resource-efficient algorithm to compute the strength. Secondly, under the settings of ICL and natural sentences, we conduct extensive experiments to validate the effectiveness of our algorithm, which not only corroborate existing findings, but also identify novel emergence patterns. Thirdly, implications for broader impacts are suggested such as the correlation between our quantification with hallucination and the feasibility to measure the emergence of closed-source LLMs.

References

- [1] J. Achiam, S. Adler, S. Agarwal, L. Ahmad, I. Akkaya, F. L. Aleman, D. Almeida, J. Altenschmidt, S. Altman, S. Anadkat, et al. Gpt-4 technical report. *arXiv preprint arXiv:2303.08774*, 2023.
- [2] S. Arora and A. Goyal. A theory for emergence of complex skills in language models. *Transactions on Machine Learning Research*, 2022. ISSN 2835-8856. Survey Certification.
- [3] Y. Bahri, E. Dyer, J. Kaplan, J. Lee, and U. Sharma. Explaining neural scaling laws. *arXiv preprint arXiv:2102.06701*, 2021.
- [4] M. A. Bedau. Weak emergence. *Philosophical perspectives*, 11:375–399, 1997.
- [5] M. A. Bedau. Downward causation and autonomy in weak emergence. 2008.
- [6] M. I. Belghazi, A. Baratin, S. Rajeshwar, S. Ozair, Y. Bengio, A. Courville, and D. Hjelm. Mutual information neural estimation. In *International conference on machine learning*, pages 531–540. PMLR, 2018.
- [7] A. Buscemi and D. Proverbio. Chatgpt vs gemini vs llama on multilingual sentiment analysis. *arXiv preprint arXiv:2402.01715*, 2024.
- [8] A. Chatterjee, K. N. Narahari, M. Joshi, and P. Agrawal. Semeval-2019 task 3: Emocontext contextual emotion detection in text. In *Proceedings of the 13th international workshop on semantic evaluation*, pages 39–48, 2019.
- [9] A. Chen. *Factuality and Large Language Models: Evaluation, Characterization, and Correction*. University of California, Irvine, 2023.
- [10] T. Computer. Redpajama-data: An open source recipe to reproduce llama training dataset, 2023. URL <https://github.com/togethercomputer/RedPajama-Data>.
- [11] J. Devlin, M.-W. Chang, K. Lee, and K. Toutanova. Bert: Pre-training of deep bidirectional transformers for language understanding. *arXiv preprint arXiv:1810.04805*, 2018.
- [12] A. Feder, Y. Wald, C. Shi, S. Saria, and D. Blei. Data augmentations for improved (large) language model generalization. In *Thirty-seventh Conference on Neural Information Processing Systems*, 2023.
- [13] E. P. Hoel, L. Albantakis, and G. Tononi. Quantifying causal emergence shows that macro can beat micro. *Proceedings of the National Academy of Sciences*, 110(49):19790–19795, 2013.
- [14] E. P. Hoel, L. Albantakis, W. Marshall, and G. Tononi. Can the macro beat the micro? integrated information across spatiotemporal scales. *Neuroscience of Consciousness*, 2016(1):niw012, 2016.
- [15] J. Kossen, Y. Gal, and T. Rainforth. In-context learning learns label relationships but is not conventional learning. In *The Twelfth International Conference on Learning Representations*, 2023.
- [16] W. Lian, B. Goodson, E. Pentland, A. Cook, C. Vong, and "Teknium". Openorca: An open dataset of gpt augmented flan reasoning traces. <https://huggingface.co/Open-Orca/OpenOrca>, 2023.

- [17] Z. Liu, Y. Liu, Z. Zhang, L. Di, F. Wei, and Y. Wang. Method for extracting power emergency plan information based on llm prompt learning. In *International Conference on Frontiers of Applied Optics and Computer Engineering (AOCE 2024)*, volume 13080, pages 106–111. SPIE, 2024.
- [18] S. Lu, I. Bigoulaeva, R. Sachdeva, H. T. Madabushi, and I. Gurevych. Are emergent abilities in large language models just in-context learning? *arXiv preprint arXiv:2309.01809*, 2023.
- [19] S. Min, M. Lewis, L. Zettlemoyer, and H. Hajishirzi. MetaICL: Learning to learn in context. In M. Carpuat, M.-C. de Marneffe, and I. V. Meza Ruiz, editors, *Proceedings of the 2022 Conference of the North American Chapter of the Association for Computational Linguistics: Human Language Technologies*, pages 2791–2809, Seattle, United States, July 2022. Association for Computational Linguistics. doi: 10.18653/v1/2022.naacl-main.201. URL <https://aclanthology.org/2022.naacl-main.201>.
- [20] S. Min, X. Lyu, A. Holtzman, M. Artetxe, M. Lewis, H. Hajishirzi, and L. Zettlemoyer. Rethinking the role of demonstrations: What makes in-context learning work? In *EMNLP*, 2022.
- [21] A. Radford, J. Wu, R. Child, D. Luan, D. Amodei, I. Sutskever, et al. Language models are unsupervised multitask learners. *OpenAI blog*, 1(8):9, 2019.
- [22] V. Rawte, S. Chakraborty, A. Pathak, A. Sarkar, S. T. I. Tonmoy, A. Chadha, A. Sheth, and A. Das. The troubling emergence of hallucination in large language models—an extensive definition, quantification, and prescriptive remediations. In *Proceedings of the 2023 Conference on Empirical Methods in Natural Language Processing*, pages 2541–2573, 2023.
- [23] F. E. Rosas, P. A. Mediano, H. J. Jensen, A. K. Seth, A. B. Barrett, R. L. Carhart-Harris, and D. Bor. Reconciling emergences: An information-theoretic approach to identify causal emergence in multivariate data. *PLoS computational biology*, 16(12):e1008289, 2020.
- [24] R. Schaeffer, B. Miranda, and S. Koyejo. Are emergent abilities of large language models a mirage? In *Thirty-seventh Conference on Neural Information Processing Systems*, 2023. URL <https://openreview.net/forum?id=ITw9edRD1D>.
- [25] R. Socher, A. Perelygin, J. Wu, J. Chuang, C. D. Manning, A. Y. Ng, and C. Potts. Recursive deep models for semantic compositionality over a sentiment treebank. In *Proceedings of the 2013 conference on empirical methods in natural language processing*, pages 1631–1642, 2013.
- [26] A. Srivastava, A. Rastogi, and e. a. Abhishek Rao. Beyond the imitation game: Quantifying and extrapolating the capabilities of language models. *Transactions on Machine Learning Research*, 2023. ISSN 2835-8856. URL <https://openreview.net/forum?id=uyTL5Bvosj>.
- [27] S. Swaminathan, A. Dedieu, R. Vasudeva Raju, M. Shanahan, M. Lazaro-Gredilla, and D. George. Schema-learning and rebinding as mechanisms of in-context learning and emergence. *Advances in Neural Information Processing Systems*, 36, 2024.
- [28] G. Team, T. Mesnard, C. Hardin, R. Dadashi, S. Bhupatiraju, S. Pathak, L. Sifre, M. Rivière, M. S. Kale, J. Love, et al. Gemma: Open models based on gemini research and technology. *arXiv preprint arXiv:2403.08295*, 2024.
- [29] Teknum. Openhermes 2.5: An open dataset of synthetic data for generalist llm assistants, 2023. URL <https://huggingface.co/datasets/teknum/OpenHermes-2.5>.
- [30] L. Wang, L. Li, D. Dai, D. Chen, H. Zhou, F. Meng, J. Zhou, and X. Sun. Label words are anchors: An information flow perspective for understanding in-context learning. In *The 2023 Conference on Empirical Methods in Natural Language Processing*, 2023. URL <https://openreview.net/forum?id=OkQD6RMUK5>.
- [31] J. Wei, Y. Tay, R. Bommasani, C. Raffel, B. Zoph, S. Borgeaud, D. Yogatama, M. Bosma, D. Zhou, D. Metzler, E. H. Chi, T. Hashimoto, O. Vinyals, P. Liang, J. Dean, and W. Fedus. Emergent abilities of large language models. *Transactions on Machine Learning Research*, 2022. ISSN 2835-8856. URL <https://openreview.net/forum?id=yzkSU5zdwD>. Survey Certification.

- [32] N. Wies, Y. Levine, and A. Shashua. The learnability of in-context learning. *Advances in Neural Information Processing Systems*, 36, 2024.
- [33] Q. Xu, Y. Peng, M. Wu, F. Xiao, M. Chodorow, and P. Li. Does conceptual representation require embodiment? insights from large language models. *arXiv preprint arXiv:2305.19103*, 2023.
- [34] J. Ye, Z. Wu, J. Feng, T. Yu, and L. Kong. Compositional exemplars for in-context learning. In *International Conference on Machine Learning*, pages 39818–39833. PMLR, 2023.
- [35] Z. Yu and Y. Dong. The emergence of a complex language skill: Evidence from the self-organization of interpreting competence in interpreting students. *Bilingualism: Language and Cognition*, 25(2):269–282, 2022. doi: 10.1017/S1366728921000870.
- [36] Z. Zeng, J. Yu, T. Gao, Y. Meng, T. Goyal, and D. Chen. Evaluating large language models at evaluating instruction following. In *The Twelfth International Conference on Learning Representations*, 2023.
- [37] M. Zhang, O. Press, W. Merrill, A. Liu, and N. A. Smith. How language model hallucinations can snowball, 2023.
- [38] X. Zhang, J. Zhao, and Y. LeCun. Character-level convolutional networks for text classification. *Advances in neural information processing systems*, 28, 2015.

A Algorithm for Estimating Mutual Information

Algorithm 1 is employed to elucidate the entire process of estimating mutual information. Simplified, the method involves two primary steps: Step 1 involves extracting representative samples from a LLM, and Step 2 entails estimating the mutual information between these representation samples. We denote the time required to estimate a pair of representations ($H_{l,t}$ and $H_{l+1,t}$) as α . Consequently, the time complexity for estimating representations from an LLM for a sequence $S_T = token1, token2, \dots, tokenT - 1$ across L block layers is denoted as $O(LT\alpha)$.

In practical implementations, α approximately costs 40 minutes on one 3090 GPU, whereas significant improvements on a 4090 GPU reduce this time to about 20 minutes.

Algorithm 1 Estimating Mutual Information

Require: : A set of input tokens $U \in \mathbb{R}^{S*T}$, where S denotes the total number of samples and T represents the number of token in each sample. A LLM f_τ with L layer of blocks and hidden state dimension D . An estimator f_θ .

Ensure: : Mutual Information $M \in \mathbb{R}^{L*T}$.

procedure 1 Extracting Representation $H \in \mathbb{R}^{S*L*T*D}$ from LLM

Initialization: $H = \emptyset$

for each sample s in S **do**

$H \leftarrow H + f_\tau(U_s)$

end for

procedure 2 Estimating Mutual Information M

Initialization: $M = \emptyset, l = 0, t = 0,$

while $l < L$ and $t < T$ **do**

$I_x \leftarrow H_{l,t}(H_{l,t} \in \mathbb{R}^{S*D})$

$I_y \leftarrow H_{l+1,t}(H_{l+1,t} \in \mathbb{R}^{S*D})$

Shuffle $H_{l+1,t}$ in the dimension S

$I_{y*} \leftarrow H_{l+1,t}(H_{l+1,t} \in \mathbb{R}^{S*D})$

$input1 \leftarrow I_x || I_y$

$input2 \leftarrow I_x || I_{y*}$

Initialization: $M_{tmp} = 0$

for Epoch $i < 10k$ **do**

$output1 \leftarrow f_\theta(input1)$

$output2 \leftarrow f_\theta(input2)$

$\mathcal{L} = \frac{1}{S} \sum_{s=1}^S (output1) - \log(\frac{1}{S} \sum_{s=1}^S (output2))$

\mathcal{L} backpropagation

if $M_{tmp} == 0$ **then**

$M_{tmp} \leftarrow -\log_2^e \mathcal{L}$

else if $M_{tmp} \neq 0$ **then**

if $M_{tmp} < -\log_2^e \mathcal{L}$ **then**

$M_{tmp} \leftarrow -\log_2^e \mathcal{L}$

end if

end if

end for

$l \leftarrow l + 1, t \leftarrow t + 1$

$M_{l,t} \leftarrow M_{tmp}$

end while

return M

B Supplementary Materials for Finding 1

B.1 Limit Number of Shots

In Section 4, we expanded the 3 categories into input sequences containing 10 shots (20 tokens each). Table 3 illustrates the changes in emergence strength for each shot relative to its predecessor within these sequences. The emergence strength of 4 different LLMs generally approached their upper limits

Model	categories	shot3	shot4	shot5	shot6	shot7
GPT2-large	country	↑5.67	↑12.95	↑2.75	↑0.33	↑1.04
	animal	↑4.24	↑6.06	↑9.52	↑0.39	↓1.44
	color	↑4.88	↑4.82	↑6.39	↑1.24	↑0.22
GPT2-XL	country	↑5.86	↑13.12	↑3.56	↑1.75	↑0.32
	animal	↑4.21	↑5.75	↑8.21	↑1.15	↑0.61
	color	↑3.82	↑4.61	↑7.06	↑1.74	↑0.54
Gemma	country	↑6.33	↑22.16	↓2.86	↑3.21	↓3.54
	animal	↑4.09	↑6.24	↑8.45	↑36.51	↓2.14
	color	↑4.65	↑5.16	↑7.81	↑16.49	↑1.21
OpenLlama	country	↑6.33	↑45.26	↑7.54	↑4.65	↓3.15
	animal	↑4.95	↑7.54	↑35.16	↑2.16	↑3.26
	color	↑4.39	↑5.27	↑27.56	↑11.42	↑2.51

Table 3: $\Delta\hat{E}(t)$ compared to the previous token. The red represents $\hat{E}(t)$ decreases compared to the previous token.

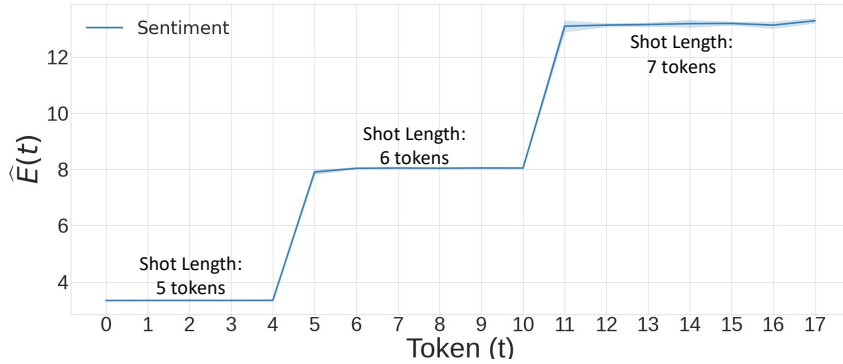


Figure 4: $\hat{E}(t)$ with inputs of 18 tokens, consisting of 3 shots in 5 tokens, 6 tokens, 7 tokens, respectively.

by the 6th and 7th shots. It is important to note that these results only indicate the existence of an upper limit to the contribution of shot quantity to emergence in ICL. They do not imply that the 6th and 7th shot universally represents the upper limit for all ICL tasks.

B.2 Shot Length

To examine the emergence strength associated with shot lengths, we designed a shot format pertinent to sentiment analysis as follows:

“[entity] sentiment: [label],”

where “[entity]” represents emotional words such as “happy,” “thrill,” “offended”, etc., and “[label]” options include “positive” or “negative,” specifically chosen based on the category of “[entity]”. The token length of “[entity]” was employed to control the overall length of the shot; for instance, when “[entity]” consists of single-token words like “anger,” “love,” etc., the entire shot spans 5 tokens, whereas for two-token words like “hopeful,” “resentful,” etc., the shot extends to 6 tokens. Consequently, we generated 300,000 input samples, each 18 tokens in length, comprising 3 shots with lengths of 5 tokens, 6 tokens, and 7 tokens respectively.

Figure 4 corroborates our hypothesis: within each shot, all tokens share a uniform emergence strength. This observation supports another intuitive viewpoint of ICL: an LLM gains greater confidence in the correctness of its predictions only when a new shot is introduced.

measure	t0	t1	t2	t3	t4	t5	t6	t7
baseline	4.69	4.69	9.46	9.37	15.32	15.02	28.44	29.47
model1	4.64	4.69	9.44	9.45	15.09	14.67	27.59	28.67
model2	4.64	4.68	9.44	9.28	15.27	14.66	44.08	36.37
model3	4.69	4.68	9.47	9.45	15.29	15.54	52.28	85.61
token1	2.82	2.83	6.88	6.85	11.08	10.95	16.83	16.09
token2	3.60	3.60	7.36	7.29	11.15	11.08	15.86	14.96
candidate	3.26	3.26	7.22	7.22	11.44	11.35	17.15	17.33
fusion1	3.84	3.84	7.63	7.64	11.66	11.49	17.45	16.28
fusion2	3.45	3.45	7.26	7.05	11.05	11.06	16.45	16.59
space	4.69	4.69	9.46	9.37	15.32	15.02	22.44	5.19
prefix	4.69	4.69	9.46	9.46	15.32	15.34	37.85	41.05

Table 4: ‘‘Ablation Study’’ of how emergence changes with different measures adopted. t0-t7 represent 1st - 8th token.

B.3 Cases of Inaccurate Generations with Excessive Shots

In Table 1 we found 2 types of erroneous repetition, we listed some cases of them from GPT2-XL, in which blue text indicates the shots as prompt, the green text indicates correct entities and red text indicates wrong entities:

Case 1: The sequence breakdown was precipitated by the output of an incorrect entity.

‘‘Ukraine, Mexico, Russia, Australia, New Zealand, United Kingdom, United States, Canada, United States of America, United States of America, United States of America, United States of America’’

Case 2: Due to a loop spanning the shots, no new entities were generated.

‘‘Canada, France, Turkey, Iran, Russia, Ukraine, United Kingdom, United States, Canada, Germany, United States, Canada, Germany, United States, Canada, Germany, United States, Canada, Germany’’

C Supplementary Materials for Finding 2

To investigate the influence of different factors on emergence strength, we treat the performance of GPT2-XL on the ‘‘country’’ dataset as a baseline and implemented a series of variations. First, we replace GPT2-XL with other LMs, namely **model1** using GPT2-large, **model2** using GEMMA, and **model3** using OpenLlama. Second, we vary the dataset, forming **data1** using ‘‘animal’’ dataset and **data2** using ‘‘color’’ dataset. In addition, we use **candidate** to denote reduced candidates in the original ‘‘country’’ dataset (reducing the total number of countries from 25 to 15), and **fusion1**, **fusion2** to denote mixed candidates where fusion 1 mixes data from ‘‘country’’ and ‘‘animal’’ domains, and fusion 2 mixes data from ‘‘country’’, ‘‘animal’’, and ‘‘color’’ domains. Last, we alter the input sequence, forming **space** by replacing the *entity* in the 4th shot with *space+entity*¹². **prefix** prepends a *comma* to the original first token.

As shown in Table 4, Differences in model emergence become apparent only when a sufficient number of shots are provided. Statistically, models with larger parameter sizes exhibit higher emergence. However, differences in data are apparent starting from the first shot, likely related to the domain of training data (token1, token2). Furthermore, depleting the diversity of shots effectively reduces the emergence effects in ICL (candidate). Lastly, the format of the prompt significantly influences emergence, explaining LLMs’ sensitivity to certain perturbations (space, prefix).

D Supplementary Materials for Finding 3

We observed variations in the emergence statistics of tokens at different positions within a sentence. Consequently, we systematically evaluated tokens at various positions within a sentence, as illustrated in Figure 5. Specifically, token0, token1, and token2 were derived from the same sample set A from

¹²In the GPT-2 tokenizer, *space+entity* is treated as a new token.

	OpenOrca						
	token0	token1	token2	token-3	token-2	token-1
with previous token	8.38	13.42	15.56		17.11	17.16	17.26
wo. previous token	8.38	10.75	10.63		10.69	10.64	12.85

	OpenHermes						
	token0	token1	token2	token-3	token-2	token-1
with previous token	7.91	12.37	15.03		18.37	18.43	19.22
wo. previous token	7.91	10.78	10.91		10.88	10.95	12.62

(a) GPT2-XL

	OpenOrca						
	token0	token1	token2	token-3	token-2	token-1
with previous token	10.53	17.27	20.17		21.27	21.66	22.41
wo. previous token	10.53	10.65	10.49		10.58	10.48	10.62

	OpenHermes						
	token0	token1	token2	token-3	token-2	token-1
with previous token	9.59	16.80	22.28		25.31	25.33	25.54
wo. previous token	9.59	9.66	9.62		9.48	9.67	9.61

(b) GEMMA

Figure 5: Mutual information of each token position in two datasets, taking GPT2-XL and GENNA as examples.

OpenOrca, while token-3, token-2, and token-1 were taken from another sample set B from OpenOrca. Sample set A ensured that token0 was the initial token of the sentence, while set B ensured that token-1 was the last token of the sentence. This allowed us to measure differences in emergence statistics for tokens at the beginning, middle, and end of sentences across variable sentence lengths.

Figure 5 presents an interesting phenomenon: taking GPT2-XL and GEMMA as examples, GPT2-XL exhibits distinct responses to tokens at different sentence positions—emergence values increase at the beginning, stabilize in the middle, and rise again at the end. GEMMA, on the other hand, does not display such positional sensitivity. We hypothesize that this may be related to the different preprocessing methods used in the training data.

E Detailed Mutual Information Tables

Tables 5 and 6 present the performance of GPT2-XL on the Animal category and OpenOrca datasets, respectively. Although “shots” and “natural sentences” demonstrate different patterns, they share a common characteristic: mutual information increases with token length, aligning well with the NTP mechanism.

layer	token0	token1	token2	token3	token4	token5	token6	token7
1	2.83	2.83	6.89	6.50	10.68	9.24	14.16	11.53
2	2.83	2.83	6.90	6.91	11.08	11.10	16.70	16.79
3	2.83	2.83	6.89	6.88	11.17	11.17	16.93	16.00
4	2.83	2.83	6.89	6.88	11.08	11.06	16.74	16.58
5	2.83	2.83	6.89	6.89	11.13	11.11	16.94	15.88
6	2.83	2.83	6.88	6.89	11.16	11.16	18.89	17.11
7	2.84	2.83	6.89	6.88	11.15	11.14	16.97	17.08
8	2.83	2.83	6.88	6.88	11.12	11.19	16.86	17.42
9	2.83	2.83	6.90	6.88	11.20	11.17	16.92	15.97
10	2.83	2.83	6.88	6.88	11.08	11.14	16.97	16.51
11	2.83	2.83	6.88	6.88	11.04	11.05	17.05	16.19

Table 5: Mutual information of GPT2-XL in Animal category. Red represents the highest value in this block.

layer	token0	token1	token2	token3	token4	token5	token6	token7
1	8.40	13.71	16.01	17.33	17.21	17.67	17.95	17.29
2	8.36	13.77	15.76	17.06	17.08	17.72	17.68	18.00
3	8.44	13.75	16.09	17.10	17.82	17.69	17.84	18.04
4	8.44	14.20	16.07	17.29	17.45	17.74	18.51	17.81
5	8.39	13.50	16.32	16.83	17.82	17.98	18.26	18.14
6	8.41	13.69	16.03	16.99	17.58	17.82	17.52	18.33
7	8.41	13.68	16.06	17.00	18.32	17.72	17.69	18.19
8	8.40	13.80	15.97	17.26	17.61	17.73	17.52	18.44
9	8.35	13.69	15.95	17.17	17.21	17.54	17.47	18.03
10	8.41	13.57	16.30	16.57	17.46	17.85	17.85	17.51
11	8.34	13.37	16.02	15.93	17.30	17.24	17.27	16.91

Table 6: Mutual information of GPT2-XL in OpenOrca dataset. Red represents the highest value in this block.